Journal of Industrial and Systems Engineering
Vol. 3, No. 3, pp 152-169
Fall 2009

JISE

A Statistical Analysis of the Aircraft Landing Process

Babak Ghalebsaz-Jeddi [1*], George L. Donohue[2], John F. Shortle[3]

[1]Fairfax, Virginia 22030
Babak.Jeddi@gmail.com

[2,3] Dept. of Systems Engineering and Operations Research, George Mason University,
Fairfax, Virginia 22030

ABSTRACT

Managing operations of the aircraft approach process and analyzing runway landing capacity, utilization and related risks require detailed insight into the stochastic characteristics of the process. These characteristics can be represented by probability distributions. The focus of this study is analyzing landings on a runway operating independent of other runways making it as a single runway. We provide statistical analysis of the final approach and runway occupancy time at Detroit airport at peak traffic periods on one of its major landing runways. Many weeks of aircraft track record data collected by a multilateration surveillance system is analyzed. We explain some characteristics and short comings of the database, and extract samples of the random variables of interest (i.e. aircraft time and distance separation, runway occupancy time, simultaneous runway occupancy, and aircraft speed). We estimate probability distributions of these variables under both instrument and visual flight rules. Although the focus here is on one runway at a large airport, probability distributions of these random variables for the landings on similar single or independent runways (with similar physical design, operating systems and landing guidance instruments) shall be alike.

***Keywords*:** Runway landing, Final approach, Aircraft separation, Landing systems, Multilateration data, Distribution fitting, Risk

1. INTRODUCTION

Runways are the main bottlenecks in the air transportation system during busy periods, and optimizing their operations (landing and departure) is critical. In the landing aspect, the utilization and safe throughput depends on the separation between any lead and trailing aircraft while approaching the runway. Separation is necessary to control two risks: simultaneous runway occupancy and hazardous encounter of trailing aircraft with the wake vortices from its leading aircraft; for some discussion about physics of wake vortex and its quantitative hazard evaluation see Shortle and Jeddi (2007), for example. Separation of an aircraft pair is a random variable due to the nature of the process inputs and components. Thus, analysis of the landing capacity, utilization and risks require detailed insight into the stochastic characteristics of the process, and we utilize statistical methods for this purpose.

* Corresponding Author

In the final phase of the approach process the aircraft typically follows a path from the Initial Approach Fix (IAF) to the Final Approach Fix (FAF) and continues to touch down on the runway, a few hundred feet from the runway threshold. The path is called the *glide slope* or *glide path* with about 3^o slope from the ground. Figure 1 shows the glide path to runway 21L (reads 21 left) at Detroit Metropolitan Wayne county airport (DTW) using Instrument Flight Rule (IFR) or Instrument Landing System (ILS). Some authors use Instrument Meteorological Condition IMC equivalent to IFR and ILS and imply that ILS is only used when the condition is IMC. However, ILS system may also be utilized in a good weather condition referred to as visual meteorological condition VMC, and some databases report the periods during which the ILS was in use. For these reasons we indicate what data/info is related to ILS use rather than indicating the weather condition. In Figure 1, IAF and FAF are 19.9 nm and 5.9 nm from the landing threshold at 7,000 ft and 2,600 ft altitudes, respectively. For the official Instrument Approach Procedures on runway 21L see FAA (2009a). Note that the 2009 approach plate is slightly different than 2002 and 2003 versions.

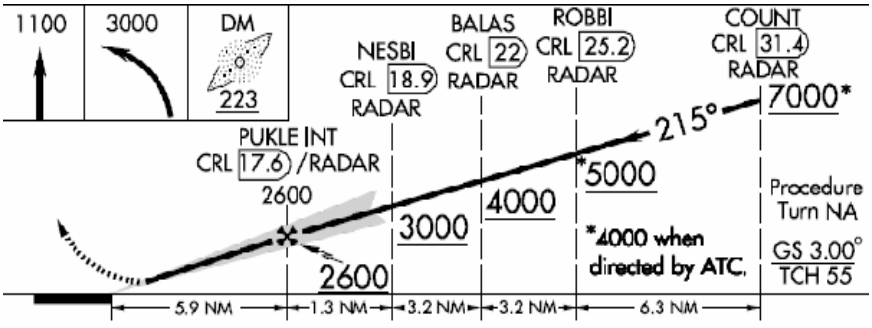

Figure 1 A Typical final approach process under ILS; Runway 21L at DTW (FAA 2009a)

The focus is on the following random variables in this study:

IAT Inter Arrival Time of consecutive aircraft to the Final Approach Fix (Figure 1)

LTI Landing Time Interval between successive aircraft at the runway threshold

IAD Inter Arrival Distance between two successive aircraft at the moment that the lead aircraft crosses the runway threshold

ROT Runway Occupancy Time; the length of time required for an arriving aircraft to proceed from the runway threshold to a point clear of the runway

SRO Simultaneous Runway Occupancy by two landing aircraft

To obtain samples of these random variables, varied databases and methods have been used. A literature survey on previous statistical studies is given in the preliminary report of our research at Jeddi *et al*. (2006) presented at International Conference for Research on Air Transportation. Here we just provide a summary of that survey in Table 1.

In recent years, multilateration systems have been installed in some airports, including Detroit Metropolitan Wayne County airport (DTW) which provide reasonably accurate time-position estimates of all transponder-equipped aircraft operating in the airport vicinity in all weather conditions. We utilize these data to obtain samples of the random variables under study.

The Center for Air Transportation Systems Research (CATSR) at George Mason University has obtained one year of multilateration surveillance system data of DTW via Volpe National Transportation Systems Center. The original multilateration data have been de-identified by Sensis Corporation, and the filtered data are used in this study. However, as discussed later, there are still some outliers, noise, and missing data present in the database. As shown in Table 1, this paper analyzes multilateration data at Detroit airport (DTW) in section 2, and provides estimations for probability distributions of *IAT*, *LTI*, *IAD*, *ROT*, *SRO,* and average approach speed in section 3. We reported some preliminary results of analyzing one week data under ILS, collectively on all runways, at Jeddi *et al*. (2006). Some of these results are further discussed in this paper whenever useful for completeness.

Table 1 A summary of related statistical studies

		Sampling database or method				Sampled variable				
Author	Airport	Stop watch	Radar track	PDARS	Multi-lateration	*IAT* at FAF	*LTI*	*IAD*	*ROT*	*SRO*
Vandavenne, Lipert, MIT 1992	DFW	√					√			
Ballin, *et al*. NASA, 1996	DFW		√				√	√		
Andrews, Robinson, MIT, 2001	DFW		√				√	√		
Haynie, CATSR, 2002	LGA, ATL	√					√		√	√
Levy, Sensis, 2004	MEM				√		√ VMC	√ VMC	√ VMC	
Rakas and Yin, Berkeley, 2005	LAX			√			√			
Xie, CATSR, 2005	LGA	√					√		√	√
This paper	DTW				√	√	√	√	√	√

2. DATA ANALYSIS

Multilateration data shall be processed to extract time and position recordings including aircraft times at the FAF, time over the runway thresholds, runway exit times, and the position of the following aircraft when the leader is over the runway threshold. We investigate aircraft data at DTW on December 2002, February 2 to 8, 2003, June 2003, and August 2003 (in Greenwich Mean Time) to provide probability distributions for the random variables of interest. The data of December 2002, June 2003, and August 2003 on runway 21L were pre-processed by V. Kumar at CATSR-GMU which makes the data ready to be directly feed into MATLAB algorithm for information recordings and data extraction. Some data queries of December 2002, June 2003, and August 2003 on runway 21L were made by V. Kumar at CATSR-GMU which we fed into our MATLAB algorithm for information recordings and data extraction.

Figure 2 is a simplified airport diagram of DTW (AirNav.com 2009) with the *X*-*Y* coordinate system of the multilateration data projected on top of it. For the official airport diagram see FAA (2009b).

2.1. Database Structure and Data Preparation

For a detailed discussion on database structure, its shortcomings and our data preparation procedure, we refer the reader to our initial report at ICRAT conference, Jeddi *et al*. (2006).

In addition to preventing simultaneous runway occupancy, the main reason for aircraft separation is to control the chance that the following aircraft may encounter the hazardous wake vortex of its lead. Wake vortices are the result of lift and depend on the weight of the generating aircraft among other parameters, Nolan (2003). Aircraft are categorized based on their maximum take-off weight. Federal Aviation Administration (FAA) considers four categories as the following three weight ranges, in addition to Boeing 757, Small ≤ 41,000 lbs, 41,000 lbs < Large ≤ 255,000 lbs, and Heavy ≥ 255,000 lbs.

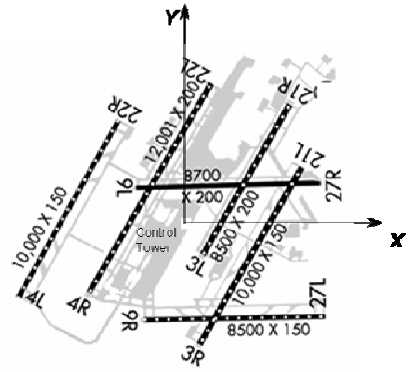

Figure 2 A simplified Detroit airport diagram with *X*-*Y* coordinates (AirNav.com 2009)

Figure 3 is the ground projection (bird's eye view) of the track plot of some aircraft landings on runway 21L (indicated at the left side of the figure) in a rotated coordinate system in which runway is aligned with the *X*-axis. The figure is expanded in the *Y*-axis for further clarity. Based on visual investigation, the noise of (*X,Y*) positions is assumed to be in an acceptable range. The FAF is at *X* ≈ 12,500m, 19.9 nm from the runway threshold (see Figure 1 and FAA 2009a).

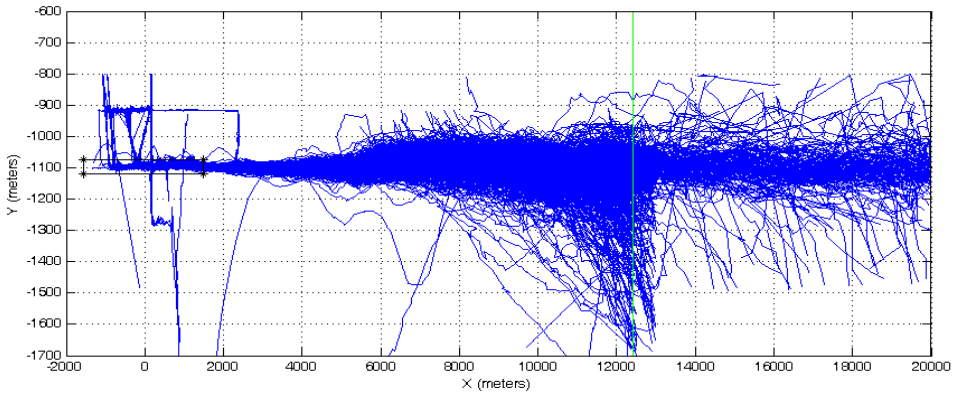

Figure 3 Some landings on runway 21L (scale of the *Y*-axis is magnified relative to the *X*-axis)

From the plotted tracks in Figure 3, it is seen that some landings follow an approach course parallel to the *Y*-axis toward the FAF. Then they cut the corner once they are about 0.5 nm from the FAF

and turn toward the runway. This study does not consider these landings and rather focuses on landings that are in the 21L direction while crossing the FAF. Almost all the collected information is conditioned on these landings in this study.

Two additional information need to be verified and combined with the track data, i.e. wake vortex weight classes of any aircraft, and the utilized landing system (IFR or VFR) in 15 min time periods. We have obtained the wake-vortex weight class of 96% of the landings under study, of which 67% are provided by Sensis Corporation and the rest are obtained by matching and search of tables of the FAA *aircraft registration* database. The utilized landing systems/rules are reported in the ASPM (Aviation System Performance Metrics) database in local time. Considering the time field of the data, we add a new field to indicate ILS/IFR and VFR landing systems.

2.2. Sample Extraction

Following the data preparation, samples of random variables are collected. Recorded data of a given aircraft might include many landings, departures, or fly-overs, but these operations are not differentiated in the database. In Jeddi *et al*. (2006), we introduced a procedure to distinguish landings from other operations, and to calculate samples of *LTI*, *IAD*, and *ROT*. The same procedure is employed in this paper.

In brief, the procedure separates different operations of any aircraft and recognizes landings on runway 21L. Then, it records the time and location of aircraft when it is first observed outside of the runway rectangle after landing, i.e. taxi-in time and location. If the aircraft track disappears over the runway, the exit from the runway is not recorded. The procedure sorts landings in an ascending manner, based on their threshold times, to recognize follow-lead aircraft. The location of any follow aircraft is recorded at the moment its lead crosses the runway threshold. The procedure calculates *ROT*, and average ground speed for any aircraft, and *IAT*, *LTI*, and *IAD* for any pair of lead-follow aircraft using the observations in previous steps. The observations are classified based on the landing system, wake-vortex weight class of the follow-lead aircraft, arrival rate, etc. We provide estimations for critical random variables in the aircraft approach process and landing.

3. LANDING STATISTICS

3.1. Landing Frequency

We define a peak period (quarter-hour) for a given runway to be the ones with at least seven landings on that runway. For the analyzed data, we have observed 14,302 landings on runway 21L in the months under study. The total 4,647 landings in peak periods are distributed among runways and aircraft types as shown in Table 2. Only 3.9% of wake-vortex weight classes of peak period landings could not be recognized. For some days in these four months, we observe no landings on runway 21L; this might be because aircraft land on other runways or the data are not collected.

Table 2 Total of 4,647 landing samples on runway 21L in peak periods

Aircraft type	Dec 2002	Feb 2003	June 2003	Aug 2003	Total	Total %
Not Available	7	8	33	133	181	3.9
Small	88	70	120	342	620	13.4
Large	367	318	720	2,148	3,553	76.5
B757	30	33	50	168	281	6.0
Heavy	2	0	1	9	12	0.3
Total	494	429	924	2,800	4,647	100

To validate that almost all landings in 15-minute periods are captured, we compared one week data of all runways of February 2-8, 2003 with the recorded landings on all runways in the ASPM database for this specific week of operations.

Figure 4 shows arrival rates per quarter hour for runway 21L. The horizontal axis is in local time. Observations start at 7:00 pm Feb 1, 2003. Shaded periods indicate ILS periods for the airport. To double check the completeness of observations in the multilateration database and to validate our data preparation and sample extraction procedure, we compare the number of landings reported in the ASPM database with the results from our study. Overall for the week of Feb 2-8, 2003, ASPM reports 160 more landings than ours. This corresponds to a small proportion of 3.6% (=100*160/4473) of ASPM records. Average and standard deviation of "Observed minus ASPM" rates are 0.24 and 1.7 arrivals per quarter-hour, respectively. This difference can be the result of missing mode-s fields, unrecorded landings, cautious in our algorithms in which tracks with questionable data are discarded, or issues related to ASPS recordings, which we are not aware of. We assume a similar pattern for the rest of the data.

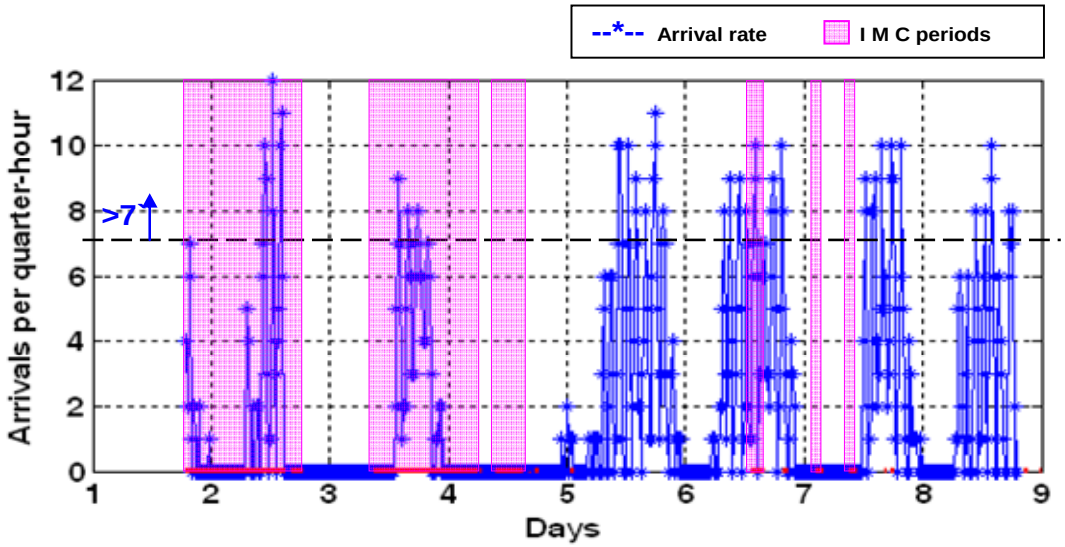

Figure 4 Arrival rates to runway 21L during Feb. 2-8, 2003, Jeddi *et al*. (2006)

For some system analysis, it is important to know the proportion of different follow-lead aircraft pairs. Table 3 shows this proportion for the data at hand in peak periods under ILS out of 852 samples. Note that these are the aircraft going through the FAF. Table 3 is also called the transition matrix. 63.3% of the pairs are large-large aircraft, and about 80% of landing aircraft are large ones.

Table 3 Follow-lead aircraft transition matrix in peak periods under ILS

Follow aircraft	Lead aircraft				
	Small	Large	B757	Heavy	Total
Small	2.0	11.4	0.5	0.2	14.1
Large	11.5	63.3	5.0	0.1	79.9
B757	1.1	4.1	0.4	0.0	5.6
Heavy	0.1	0.2	0.0	0.0	0.3
Total	14.8	79.0	5.9	0.3	100

3.2. Distributions of *IAT*, *LTI*, and *IAD*

In risk and capacity analysis, the pattern of the approach process in peak periods is of interest. For this reason, we focus on periods during which there are seven or more landings per quarter hour, i.e. peak periods.

Table 4 shows the default standard for the *approach in-trail threshold separation minima* under IFR put forth by the FAA. We are interested to know what the probability distributions of *IAT*, *LTI* and *IAD* are for class of follow-lead aircraft with the 3 nm and 4 nm separation spacing minima indicated in Table 4, i.e. pairs S-S, L-S, B757-S, H-S, L-L, B757-L, and H-L for 3 nm, and S-L, L-B757, B757-B757, and H-B757, where S stands for small, L for large, and H for heavy aircraft. In specific situations, 3 nm spacing standard may be reduced to 2.5 nm based on FAA (1993a and 1993b); however, differentiating these situations is not the subject of this study.

Table 4 IFR approach in-trail threshold separation minima (nm)

Follow aircraft	Lead aircraft			
	Small	Large	B757	Heavy
Small	3	4	5	6
Large	3	3	4	5
B757	3	3	4	5
Heavy	3	3	4	4

We have collected a significant number of samples from the variables of interest under ILS/IFR and VFR. Independence of samples is necessary to fit probability distributions. This independence is examined by *lag analysis* and test of hypothesis. A *one-lag scatter plot* is shown in Figure 5 for *LTI* 3 nm, i.e. *LTI3*. The plot does not demonstrate a specific pattern of dependency between consecutive samples.

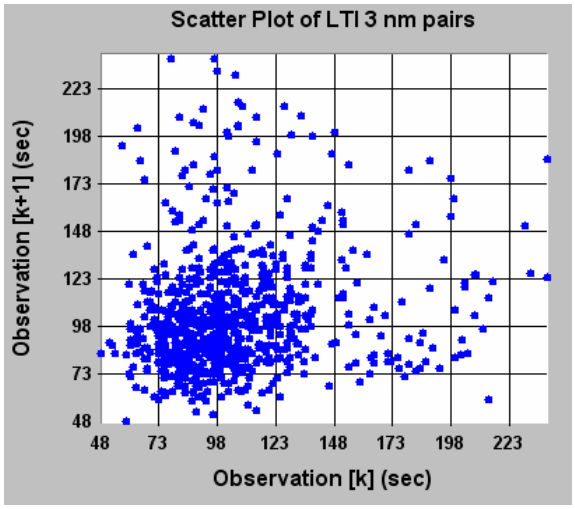

Figure 5 One-lag scatter plot of peak-ILS period *LTI* for 3 nm pairs; no specific pattern is observed

Table 5 shows one and two lag autocorrelation coefficients and p-values for the two lag test of hypothesis for variables of interest under ILS. For more information on statistical concepts discussed in this paper, see Bowker and Liberman (1972), for example.

Table 5 Autocorrelations and p-values for the variables under ILS

Variable	*IAT3*	*IAT4*	*LTI3*	*LTI4*	*IAD3*	*IAD4*
One-lag autocorr.	0.124	0.162	0.121	0.16	0.133	0.043
Two-lag autocorr.	0.04	0.001	0.041	0.016	0.103	-0.028
p-value for two-lag	0.24	0.987	0.255	0.843	0.005	0.730

The one-lag autocorrelations are small and do not imply dependency although in some cases they exceed 0.1. The two-lag autocorrelations are much smaller. We perform hypothesis tests on two-lag autocorrelations to examine data independence. Based on p-values we cannot reject sample independence for none of the variables in 99% confidence level except for *IAD3*. Three-lag auto-correlation coefficient for *IAD3* samples is 0.015 and the corresponding p-value is 0.68, i.e. cannot reject sample independence hypothesis in three-lag analysis. A weak one-lag and two-lag linear dependencies among the samples do not imply interdependency among all data.

The number of samples, minimum and maximum values, mean and standard deviation of the samples for each variable for both 3 nm and 4 nm pairs under ILS are given in Table 6. We use ExpertFit, Law (2000), and MATLAB packages for distribution fitting. The method of Maximum Likelihood Estimation (MLE) is used for these fittings. A few samples with *LTI3* or *IAT3* greater than 300 s are truncated as large separations are not safety concerns, and may reduce the fitting accuracy as the sample domain increases. Interestingly, for all of the variables, the shifted log-logistic distribution provides the best fit. Figure 6 provides histogram and two best fitted pdf for *LTI3* under ILS.

Table 6 Estimated landing distributions under ILS on runway 21L in peak periods

ILS/IFR Variable	Sample values				Fitted values					
	Size	[min,max]	Mean	Std	Distribution	Shift	Scale	Shape	Mean	Std
IAT3 at FAF (s)	772	[53,218]	105	30.5	Log-Logistic	50	48.45	3.46	106	35.7
LTI3 (s)	770	[48,295]	104	30.6	Log-Normal	40	4.06	0.45	104	30.4
					Log-Logistic	45	52.30	3.60	105	36
*IAD3** (nm)	756	[1.9,10.0]	3.6	1.1	Log-Logistic	1.8	1.54	3.25	3.6	1.3
IAT4 at FAF (s)	162	[65,250]	121	33.5	Log-Logistic	60	53.84	3.25	123	44.8
LTI4 (s)	162	[70,243]	124	33.2	Log-Normal	65	3.99	0.31	125.1	35
					Log-Logistic	65	52.2	3.48	125	38.1
IAD4 (nm)	152	[2.4,9.5]	4.1	1.1	Log-Logistic	1.3	2.61	5.26	4.1	1.0
IAT5 at FAF (s)	6	[120,134]	128	6.2	Not fitted					
LTI5 (s)	6	[120,147]	131	9.0	Not fitted					
IAD5 (nm)	6	[3.9,5.1]	4.6	0.4	Not fitted					
IAT6 at FAF (s)	2	[148,167]	158	13.4	Not fitted					
LTI6 (s)	2	[158,162]	160	2.8	Not fitted					
IAD6 (nm)	2	[5.6,6.1]	5.9	0.4	Not fitted					

* Samples demonstrate some linear dependency in one and two lag.

As given in Table 6, the probability distribution of *LTI3* can be well estimated by a log-normal distribution with parameters (40; 4.06, 0.45) when a minimum of 40 seconds is enforced. The log-logistic(45; 52.30, 3,3.6) provides a slightly better fit relative to the log-normal distribution. The fit is accepted by a Kolmogorov-Smirnov test (KS-test) for significance levels of 0.05 or smaller. Note that log-logistic distribution has a heavier tail than log-normal distribution. For example, P(*LTI3*>240) is 0.003 and 0.004 when it is respectively fitted by log-normal and log-logistic distributions. The heavier tail of log-logistic distribution causes a higher standard deviation as seen in Table 6, but it is not a concern as it only related to the tail of the distribution.

One-lag autocorrelation coefficients of samples for the variables under VFR are given in Table 1. Except for *IAD3* and *IAD4*, the values are very small and demonstrate sample independence. Based on p-values, we cannot reject sample independence for none of the variables in 99% confidence level except for *IAD3*. Two-lag autocorrelation coefficient for *IAD3* samples is 0.089 and the corresponding p-value is 0.0003, i.e. rejected the hypothesis of two-lag sample independence. Three-lag auto-correlation coefficient for *IAD3* samples is 0.044 and the corresponding p-value is 0.09, i.e. cannot reject sample independence in three-lag analysis. A weak one-lag and two-lag linear dependencies among samples of *IAD* do not imply interdependency among all data. We observe more sample independence under VFR than under IFR.

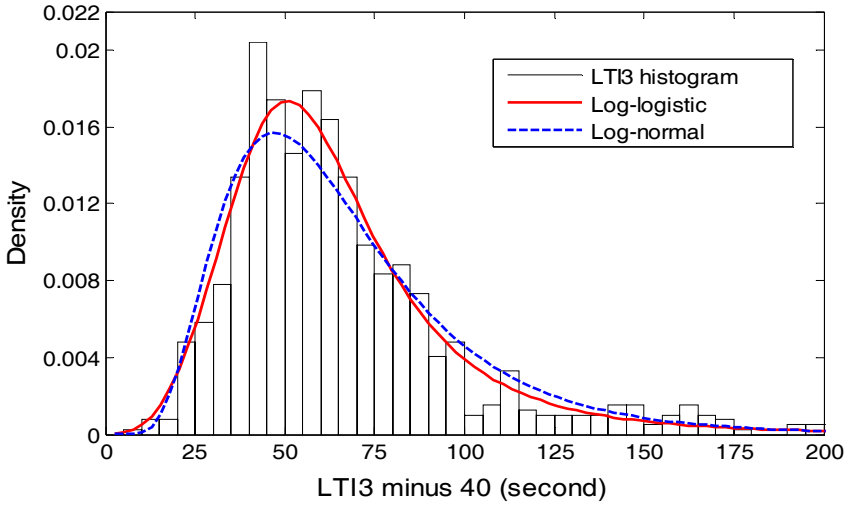

Figure 6 Histogram and estimated distribution of peak period *LTI*3 under ILS; Log-logistics is a better fit

Table 7 One-lag autocorrelation coefficients and p-values under VFR

Variable	*IAT3*	*IAT4*	*LTI3*	*LTI4*	*IAD3*	*IAD4*
One-lag autocorr.	0.001	0.008	0.009	0.013	0.133	0.14
p-value	0.962	0.887	0.724	0.813	0.000	0.017

Table 8 is the summary of the collected samples under VFR and corresponding estimated probability distributions for the random variables of 3, 4, and 5 nm separation minima pairs from Table 4. There are two points of 28 s and 33 s for *IAT3* at FAF where their *LTI3* at the threshold are 77 s and 89 s, respectively, which are much larger (and more reasonable) than their *IAT*; we consider these two points as outliers and drop them from the data.

Table 8 Estimated landing distributions under VFR on runway 21L

VFR variable	Sample values				Fitted values					
	Size	[min,max]	Mean	Std	Distribution	Shift	Scale	Shape	Mean	Std
IAT3 at FAF (s)	1618	[40,236]	102	32	Log-Logistic	39	55.84	3.78	102	35.4
LTI3 (s)	1623	[39,233]	102	32	Log-Normal	38	4.04	0.47	102	31.6
					Log-Logistic	38	56.26	3.85	101	34.7
*IAD3** (nm)	1539	[1.5,9.2]	3.5	1.0	Log-Logistic	1.3	1.74	3.82	3.5	1.1
IAT4 at FAF (s)	331	[48,231]	116	30	Log-Logistic	45	66.40	4.13	118	36.7
LTI4 (s)	336	[56,238]	121	31	Log-Normal	50	4.16	0.47	122	35.6
					Log-Logistic	50	65.44	4.00	123	38
IAD4 (nm)	306	[1.6,7.0]	4.1	0.9	Log-Logistic	1.7	2.23	4.24	4.1	1.2
*IAT5*** at FAF (s)	27	[76,223]	133	39	Log-Normal	75	3.67	1.13	149	120
*LTI5*** (s)	27	[81,227]	138	36	Log-Normal	75	3.90	0.82	144	68
*IAD5*** (nm)	24	[2.7,6.8]	4.7	1.2	Log-Normal	2.5	0.58	0.76	4.9	2.1
IAT6 at FAF (s)	3	[132,228]	176	48.4	Not fitted					
LTI6 (s)	3	[142,277]	203	68.3	Not fitted					
IAD6 (nm)	2	[5.45,5.5]	5.5	0.03	Not fitted					

* Samples demonstrate some linear dependency in one and two lag.
** Fitted distributions are not reliable because of the small sample size

From Table 8, note that the mean of *LTI5* is 17 s more than mean of *LTI4*, and mean of *LTI4* is 19 s more than mean of *LTI3*. Means of *IAD4* and *IAD3* differs only by 0.5 nm, and means of *IAD5* and *IAD4* differs by 0.6 nm. Standard deviations are almost identical between corresponding 3 nm and 4 nm pairs, but it is slightly higher for 5 nm pairs in average.

Figure 7 shows histogram of *IAT5* (shifted to the left by 75 s) and two fitted distributions of log-normal and log-logistic. Because of very limited samples on the wide domain, no fitting can be suitably representative of the population distribution. Standard errors for scale and shape parameters for the estimated log-normal distribution are 0.18 and 0.13, i.e. 5% and 16% of the estimated values, respectively. The standard deviation of *IAT5* is 120 s based on the estimated distribution where as the sample variance is 39 s.

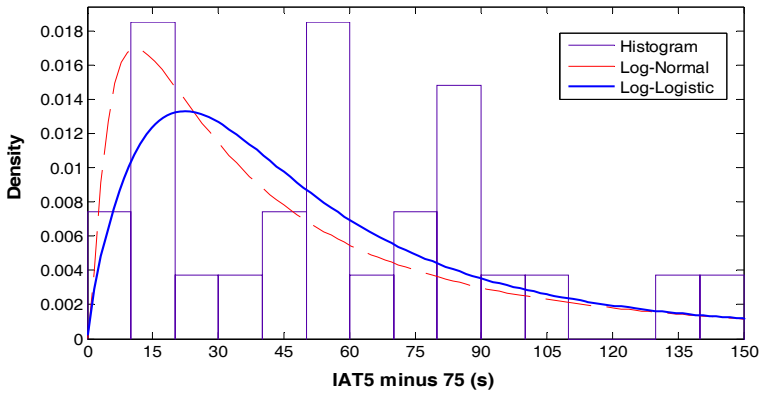

Figure 7 Two fitted distributions on the *IAT5* histogram

3.3. Distribution of *ROT* under ILS

For theoretical estimation of the simultaneous runway occupancy risk, we need to estimate the probability distribution of the *ROT*. As we see from the airport diagram, 21L has 4 exits (taxi-ways), two of which are prior to the half-way of the runway and two others are after that. This suggests that some fraction of the aircraft exit early and some exit later. This is also supported by the histogram of *ROT* samples of small and large aircraft, representing landings of leading aircraft of 3 nm pairs in Table 4. We condition the data on early exits (X ≥ -400 m) and late exits (X < -400 m) based on the taxi-way locations. The total sample size of *ROT* under ILS is 1,098. The one-lag and two-lag correlation coefficients among these samples are 0.044 and 0.075, respectively, which support that the samples are almost independent.

For the mix of small and large aircraft, which form the 3 nm pairs, having 1,029 samples under ILS, we observe that 62% of the landings exit the runway in early taxi-ways, and 38% exit from the later taxi-ways. We dropped samples of *ROT* < 20 s, so the data range is [24, 98]. Aircraft weight classes of thirty one of the samples, in the range of 24 s and 33 s, could not be recognized. However, because of their small values, we assume they are either small or large aircraft (i.e. they could not be B757 or heavy aircraft).

The beta distribution might be preferred for *ROT* because, as in real situations for *ROT*, it has lower and upper bounds. For both the early and late exits, the normal distribution is rejected in the 0.10 significance level.

We estimated distributions of early *ROT* and late *ROT* by beta distributions as shown in Figure 8, and Table 9. Collective pdf of *ROT* under ILS for the mix of small and large aircraft is given by 0.62∗(pdf of early exits) + 0.38∗(pdf of late exits), or

$$ROT_{S,L} \sim 0.62 \text{ Beta } ([20,90], 11.23, 26.33) + 0.38 \text{ Beta } ([30,110], 13.60, 27.39). \quad (1)$$

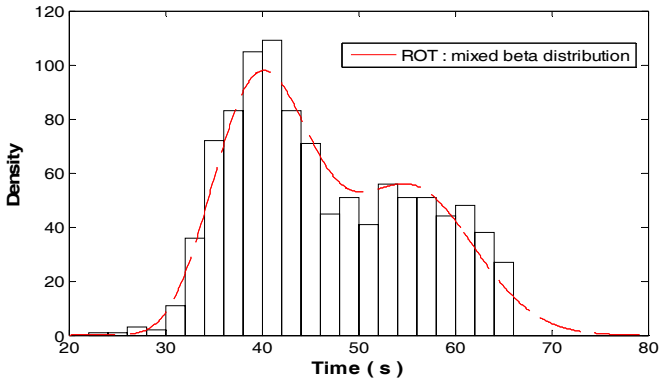

Figure 8 Histogram and pdf of *ROT* for the mix of small and large aircraft

Table 9 also shows the 95% confidence intervals on each parameter. The mean and variance of beta([*L, U*]; *α, β*) are respectively given by

$$\mu = L + (U - L) * \frac{\alpha}{\alpha + \beta} \quad \text{and} \quad \sigma^2 = (U - L)^2 * \frac{\alpha\beta}{(\alpha + \beta)^2 (\alpha + \beta + 1)}, \quad (2)$$

where L and U are the lower and upper limits of the distribution domain. Using equation (2), mean and standard deviations of each estimated distribution is calculated in Table 9. The aggregated sample of early and late exits has the mean of 47 s and standard deviation of 9.3 s, almost identical with the mixed beta distribution.

Table 9 Distribution parameters of *ROT* for the mix of small and large aircraft

	Data range	Sample size	Domain	%	α	95% C.I. for α	β	95% C.I. for β	Dist. mean	Dist. Std
Early	[24,63]	638	[20,90]	62	11.23	[10.3,12.1]	26.33	[24.2,28.5]	41	5.2
Late	[35,66]	391	[30,110]	38	13.60	[12.2,15.0]	27.39	[24.1,30.6]	58	5.8
Total		1029		100					47.5	

For the mix of large, B757, and heavy aircraft, which form pairs of 4 nm and 5 nm separation minima in Table 4, we have 910 samples under ILS. The estimated distribution is slightly different from the previous case as expected more aircraft exit later. The estimated mix beta parameters and confidence intervals are given in Table 10.

Table 10 Distribution parameters of *ROT* for the mix of large, B757, and heavy aircraft

	Data range	Sample size	Domain	%	α	95% C.I. for α	β	95% C.I. for β	Dist. mean	Dist. Std
Early	[38,63]	452	[25,90]	49.7	15.75	[13.8,17.7]	40.24	[36.0,44.4]	43.5	3.9
Late	[35,98]	458	[30,110]	50.3	8.31	[7.6,9.0]	14.72	[13.5,15.9]	60	7.8
Total		910		100					51	

In short, we can write this distribution as

$$ROT_{L,B757,H} \sim 0.497\ \text{Beta}([25,90], 15.75, 40.24) + 0.503\ \text{Beta}([30,110], 8.31, 14.72). \quad (3)$$

Distribution of *ROT* depends on the fleet mix as smaller aircraft exit earlier and larger ones later.

3.4. Average ground speed under ILS

Time and distance separation directly relate by speed. The ground speed through the final approach depends on the headwind; as the headwind is higher, aircraft needs less thrust to maintain the necessary lift. Table 11 is the summary of the observed samples of average ground speed for different types of aircraft from the FAF to the runway threshold when ILS in use.

Table 11 Average aircraft speed (in knots) from the FAF to the runway threshold under ILS

Aircraft type	Size	Domain	Mean	Std	Fitted dist.	shift	scale (standard error)	shape (standard error)	Mean	Std
Small	155	[90, 156]	125.2	13.9	Logistic	70	55.6 (1.1)	7.9(0.5)	125.6	14.3
Large	841	[80, 183]	132	14.4	Logistic	70	62.0 (0.5)	7.9 (0.2)	132.0	14.4
B757	64	[91, 163]	127	12	Logistic	80	47.3 (1.5)	6.7 (0.7)	127.3	12.1
Heavy	3	[121,160]	140	6.5	N/A					

As small standard errors of the estimated parameters show, logistic distribution provide a good fit for the speed data especially for the large aircraft. Distributions for the speed of large and small

aircraft only differ in the location parameters by 6.5 knots and maintain the shape. Figure 9 shows the histogram and fitted logistic(70; 62,7.9) distribution for the average speed of large aircraft under ILS.

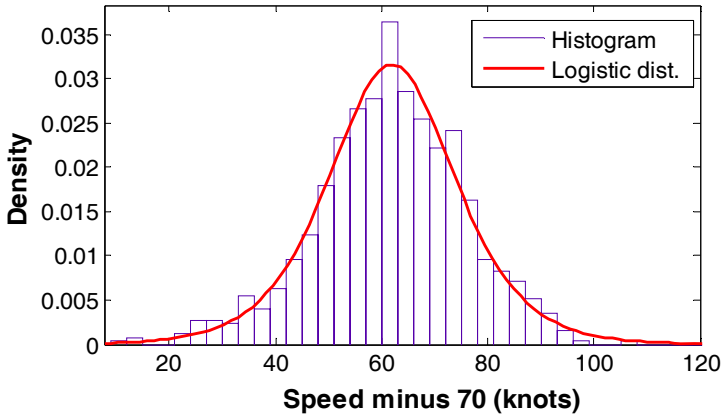

Figure 9 Histogram and fitted logistic distribution for the average speed of large aircraft under ILS

We shall note that the data demonstrate a linear dependency in one, two, and three lags as the autocorrelation coefficients are 0.63, 0.60, and 0.54, respectively. This, however, is not surprising since given the same headwind, same size aircraft land with a very similar ground speed. In other words, the observed ground speed variability is partly the result of the headwind variability. Autocorrelation coefficient of small aircraft samples in one, two, and three lags are 0.63, 0.42, and 0.31, respectively. These values are 0.48, 0.26, and 0.10 for B757 aircraft respectively.

3.5. Simultaneous Runway Occupancy

An SRO occurs when a trailing aircraft arrives at the runway threshold before its lead is clear of the runway. This is a landing risk and a precursour for a runwy incurssion. We estimate the risk of SRO by the probability (or frequency) that the *LTI* between two consecutive aircraft is less than the *ROT* of the leading aircraft, i.e. the fraction of pairs for which $\{LTI_{k,k+1} < ROT_k\}$, $k = 1, 2, \ldots$, where the leading and its trailing aircraft are respectively indexed by k and k+1.

Figure 10 shows sample observation pairs ($LTI_{k,k+1}$, ROT_k) during the week of Feb 2-8, 2003, in peak periods. The majority of these landings are on runways 21L/03R and 22R/04L, Jeddi et al. (2006). We have limited *LTI* in the figure to 200 seconds for the purpose of clarity. In this figure, pairs of follow-lead aircraft are differentiated based on the utilized landing systems ILS/IFR and VFR. Three points above the 45 degree line (where $LTI_{k,k+1}$ is less than ROT_k) correspond to SROs, one of which occurred under ILS.

Figure 10 also demonstrates the independence of $LTI_{k,k+1}$ and ROT_k for all k. The Kendall *sample-correlation statistic*, which measures dependency in non-parametric statistics, is 0.085 which is very smal and supports independence of these random variables; for discussion on this parameter see Hollander and Wolf (1999). The sample correlation coefficient is 0.15 which supports that sample dependency is very weak or does not exist. We assume the independence. In the next two sections we provide an empirical and a theoretical *point estimates* for $P\{LTI_{k,k+1} < ROT_k\}$, $k = 1, 2, \ldots$, in peak periods for pairs of aircraft with separation standard 3 nm and 4 nm indicated in Table 4.

P{SRO}: Empirical Estimation

There are totally 14 points where *LTI* < *ROT*, i.e. above the 45 degree line. The sample frequency is 0.0021 with respect to 6,832 peak period landings (the frequencies in Table 2 plus the landings that do not go through the FAF; see Figure 3). There were some landings for which we could not obtain the *ROT* due to disappearance of the aircraft track over the runway. This might be because the aircraft turned off the transponders or for other reasons. We assume that these landings would not cause SRO, i.e. would not be above the 45 degree line in the figure. On the other hand, some landings might have not been recorded by multilateration surveilence because of the errors in recording and off transponders. Thus, these are optimistic and lower bound estimations.

We build a confidence interval using the observations. Occurance of SRO is a rare event, so *SRO* can be estimated as a Poisson random variable. The Poisson random variable with parameter λ is a limit for the binomial(*n*,*p*) when *n* is large and *p* is small enough so that *np* is of moderate size, Ross (2007). Then the 95% C.I. for P{SRO} on this runway, under ILS, is [0.0011, 0.0034]. If we define an SRO to be a situation where the ROT is at least two seconds more than the landing time interval, then we have 6 SROs and the point estimation will be 0.0009 and the 95% C.I. will be [0.0003,0.0019]. These estimations are very close to our priliminary estimations using one week Feb 2-8, 2009 collective data on all runways reported at Jeddi *et al*. (2006), and Figure 10; that was 1 out of 625 under ILS, which results in a point estimation of 0.0016 which is close to the overall estimation of 0.0021 in this study.

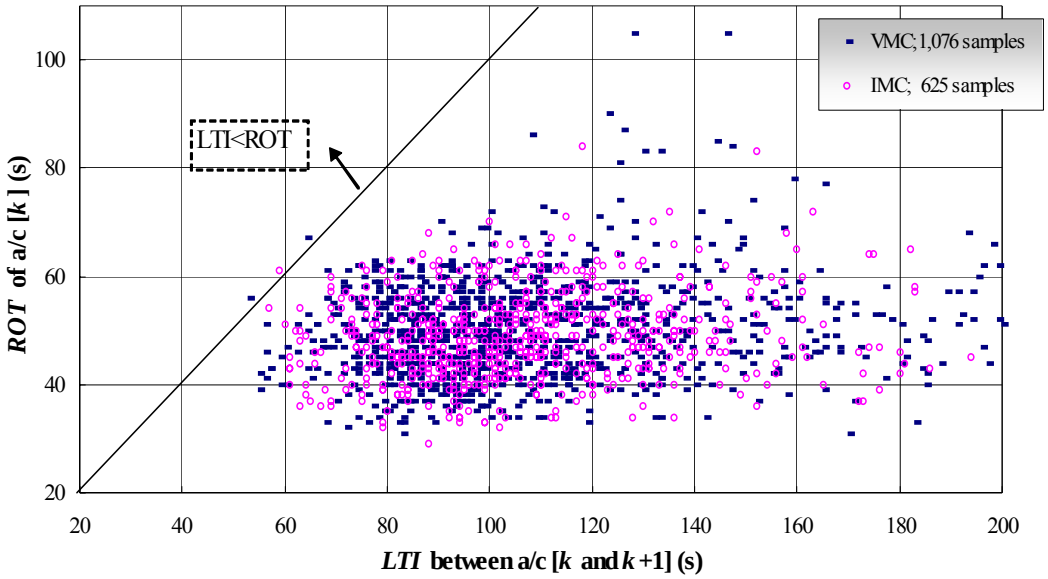

Figure 10 *ROT* of aircraft *k* versus LTI between aircraft *k* and *k*+1 during Feb 2-8, 2003, Jeddi *et al*. (2006)

P{SRO}: Theoretical Estimation

In this method the fitted probability distributions of *LTI* and *ROT* are utilized. It can provide an estimate of the overall performance of the system in its stable condition assuming the number of samples is large enough to provide a sufficient accuracy. An advantage of this method is that it covers the missing data assuming the available data captures the stable behavior of the system. As a result the estimated risk in this method might be more realistic given those assumptions. However,

noting Figure 7, we suspect that the estimated *ROT* distribution may provide over estimation of SRO for large *ROT*.

Probability distributions for *LTI*3 and *ROT* are given in Table 6 and equation (1) for 3 nm pairs under ILS/IFR. Figure 11 shows these pdfs. The observed overlap of these probability distributions suggests that P{*LTI*<*ROT*} is a positive value. In estimating pdf of *LTI*, we have not considered *LTI* samples for which we could not obtain their corresponding *ROT*. Let $g_{ROT}(\cdot)$ represent the pdf of *ROT*, and $F_{LTI}(\cdot)$ represent the cumulative distribution function (cdf) of *LTI*. Then,

$$\begin{aligned} P\{LTI < ROT\} &= \int_{-\infty}^{\infty} P\{LTI < ROT \mid ROT = x\} \cdot g_{ROT}(x)dx \\ &= \int P\{LTI < x\} \cdot g_{ROT}(x)dx \\ &= \int F_{LTI}(x) \cdot g_{ROT}(x)dx. \end{aligned} \tag{4}$$

Equation (4) cannot be evaluated analytically for the specific distributions at hand but we accurately estimate it using numerical integration; another method can be stochastic simulation which we have used to validate our numerical calculation. The result is 0.0034, as a point estimate for the pairs of interest in peak-ILS periods. (This probability will be 0.0037 if log-logistics is used instead of log-normal for *LTI3*.) As a Heuristic estimation, assuming SRO a rare event with a Poisson distribution, and assuming that this is identical to the case of observing 23 SRO out of 6832 landing, then a 95% C.I. for P{SRO} is [0.0021, 0.0051]. Note that the confidence interval for the Poisson distribution is tighter as the number of SRO observations increases, e.g. 23 in 6,832 provide a tighter C.I. than its equivalent proportion of 3.4 in 1000. Here, we have normalized the theoretical estimation of C.I. for 6,832 samples based on the empirical case.

The theoretical estimate 0.0034 is about 1.5 times the empirical estimate 0.0021 for peak-ILS periods. The empirical estimates are optimistic because firstly we have missed about 3.5% of total landing data based on the ASPM and because we could not obtain *ROT* for some peak period ILS landings. These two effects may have added to P{*LTI*<*ROT*}, i.e. they may have had bigger *LTI* than *ROT* of their leading aircraft. Based on the fitted distributions and assuming the independence of *LTI3* and *ROT*, the system performed so that the chance of SRO was in [0.0021, 0.0051] range of 95% confidence interval with the mean 0.0034.

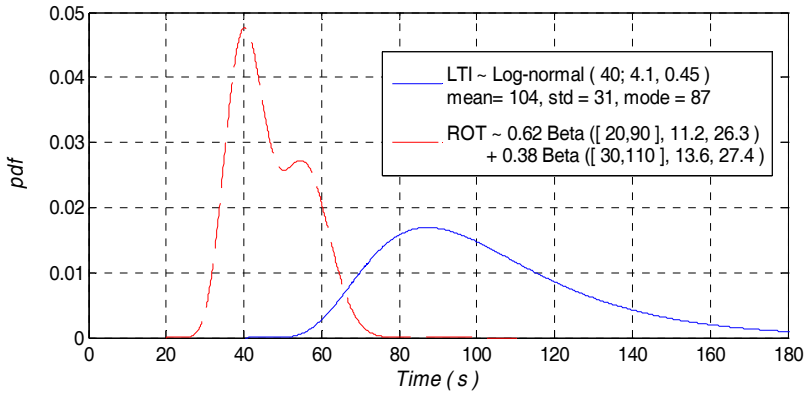

Figure 11 Overlap of *ROT* pdf and *LTI3* pdf

This empirical observations and theoretical overall estimations of P{SRO} are important indicators. The risk magnitude of P{SRO} is meant to be very small; however, based on our empirical and theoretical estimations it is 0.0021 or 0.0034, respectively, which seems to be higher than a desired value in average.

As for 4 nm pairs, having *LTI4* from Table 6 and *ROT* from equation (4), the point estimation of P{*LTI*<*ROT*} is calculated as large as 0.0006. This value is expectedly far lower than the *LTI3* case since *LTI* for the 4 nm pairs are higher than for 3 nm pairs, noting that the pdf of *LTI4* starts at 65 s.

4. CONCLUSION

We analyzed the aircraft track data from multilateration surveillance system to estimate probability distributions of approach process taking into account noise, errors, and missing data. We obtained the wake vortex weight class for 98.6% of aircraft landing in peak periods. This information is added to the multilateration data along with the information on the utilized flight rules/systems in every quarter hour obtained from the ASPM database. We extracted samples of *IAT* at the final approach fix FAF, *LTI*, *IAD*, and *ROT* during peak traffic periods in which there were seven or more landings per quarter hour on a major landing runway. We focused on runway 21L operated as an independent single landing runway. This paper extended our initial report where some statistics of the aircraft approach on all runways collectively were presented, Jeddi *et al*. (2006). Samples were additionally conditioned on weight class of follow-lead aircraft and aggregated for the ones with a minimum separation standard of 3 nm and 4 nm, whereas the initial report was only about 3 nm pairs under ILS.

The underlying process and autocorrelation analysis of the samples do not show dependency among the samples of *IAT*, *LTI*, and *ROT*. Autocorrelation coefficient showed some linear dependency in one and two lags of *IAD* samples but the independence hypothesis could not be rejected in three-lag.

We estimated the pdf of *IAT* at the FAF, *LTI*, *IAD*, and *ROT* by some known probability distributions and compared their performance. Probability distribution of *ROT* is better approximated by a mix-beta distribution but not with a normal distribution. *IAT*, *LTI* and *IAD* of the follow-lead pairs under study were best fit by log-logistic distributions; however, the log-normal distribution is also a suitable fit for *LTI3 and LTI4* under both ILS/IFR and VFR.

We estimated average ground speed of aircraft through the final approach for different aircraft types. Samples demonstrate a linear dependency because the ground speed is naturally depends on the headwind and as a result consecutive aircraft would have similar speeds. Some part of the speed variability is related to the variability of the headwind in different periods. We also showed that logistic distribution is suitable to represent the uncertainty in the average aircraft speed from the FAF to the runway threshold. We provided fitted parameters of Logistic distribution for average ground speed of small, large and B757 aircraft.

We observed that the *LTI* between the leading and following aircraft are not linearly dependent with *ROT* of its leading aircraft when all samples were analyzed collectively. The distribution of simultaneous runway occupancy *SRO* as a rare event can be estimated by Poisson distribution. The probability of SRO, P{*LTI* < *ROT*}, in peak periods are estimated empirically and theoretically by point and interval estimations, where theoretical method provides 0.0034 which is 2 times higher than the empirical estimation in average.

Providing methodologies to incorporate incomplete (*LTI*, *ROT*) data where *ROT* is missing can be of a research interest as it assists a better empirical estimation of SRO. Distribution of other random variables in the approach process, such as time between exits from the runway, and inter arrival times to the terminal radar approach control (TRACON) area can be research subjects.

DISCLAIMER

This paper represents the opinions of the authors and does not necessarily reflect the opinion of the organizations that funded or supported the study.

ACKNOWLEDGEMENT

This research was partly supported by NASA under the grant NNL05AA11G and we are grateful of that. We also thank the Volpe National Transportation Systems Center and Sensis Corporation for help in acquiring and understanding the multilateration and supporting data. We appreciate the following individuals for their support or comments: Wayne Bryant, Timothy Hall, Edward Johnson, Ben Levy, and Lance Sherry. We would like to appreciate comments and critique of referees of the JISE.

REFERENCES

[1] Andrews J.W., Robinson J.E. (2001), Radar-based analysis of the efficiency of runway use; *AIAA Guidance, Navigation and Control Conference*; AIAA-2001-4359 (Vol. 3).

[2] Ballin M.G., Erzberger H. (1996), An analysis of landing rates and separations at the Dallas/Fort Worth International Airport; *NASA Tech-Memo110397*.

[3] Bowker A.H., Lieberman G.J. (1972), Engineering Statistics; 2nd Ed, Prentice-Hall, Inc.

[4] FAA Order 7110.65 (1993a), Air Traffic Control., Wake Turbulence, Para 2,1,19, , September.

[5] FAA Order 7110.65 (1993b), Same Runway Separation, September 1993, Wake Turbulence, Para 3,9,6, , September.

[6] Haynie C.R.(2002), An investigation of capacity and safety in near-terminal airspace for guiding information technology adoption; *Ph.D. dissertation, Department of Systems Engnineering and Operations Research*; George Mason University, Fairfax, VA.

[7] Hollander M., Wolf D.A. (1999), Nonparametric statistical methods; 2nd Ed., John Wiley & Sons, Inc.

[8] Jeddi B., Shortle J., Sherry L. (2006), Statistics of the approach process at Detroit metropolitan Wayne county airport; *Proceedings of the 2nd International Conference on Research in Air Transportation (ICRAT)*, Belgrade, Serbia and Montenegro.

[9] Law A.M. (2000), ExpertFit, Averill M. Law & Associates.

[10] Levy B., Legge J., Romano M. (2004), Opportunities for improvements in simple models for estimating runway capacity; *23rd Digital Avionics Systems Conference (DASC)*, Salt Lake City, UT, October.

[11] Nolan M.S. (2003), Fundamentals of air traffic control; 4th Ed., Brooks/Cole Publishing Company.

[12] Rakas J., Yin H. (2005), Statistical modeling and analysis of landing time intervals: case study of Los Angeles International Airport, California, Transportation Research Record; *Journal of the Transportation Research Board* 1915; 69-78.

[13] Ross S.M. (2007), Introduction to probability models; 9th Ed., Amsterdam; Boston, Academic Press.

[14] Shortle J.F., Jeddi B.G. (2007), Using Multilateration Data in Probabilistic Analysis of Wake Vortex Hazards for Landing Aircraft; *Transportation Research Record*; DOI: 10.3141/2007-11.

[15] Vandevenne H.F., Lippert M.A. (2000), Using maximum likelihood estimation to determine statistical model parameters for landing time separations; 92PM-AATT-006, March.

[16] Xie Y. (2005), Quantitative analysis of airport runway capacity and arrival safety using stochastic methods; *Ph.D. dissertation, Department of Systems Engineering and Operations Research*; George Mason University, Fairfax, VA.

[17] AirNav.com; *http://airnav.com/airport/KDTW*; January 2006.

[18] FAA, AL119, ILS or LOC RWY 21L; *http://204.108.4.16/d-tpp/0910/00119IL21L.PDF*; October 2009a.

[19] FAA, AL119, Detroit Metropolitan Wayne County (DTW), Airport diagram, 09127; *http://204.108.4.16/d-tpp/0910/00119AD.PDF*; October 2009b.